Progress In Electromagnetics Research C, Vol. 53, 45–53, 2014

T-Shaped Antenna Loading T-Shaped Slots for Multiple band Operation

Tao Ni*, Yong-Chang Jiao, Zi-Bin Weng, and Li Zhang

Abstract—The method of a T-shaped antenna loading T-shaped slots for multiple band operation is presented in this paper. Inspired by the fractal antenna, the proposed method is intended to be used for designing multiple band antennas. Through loading T-shaped slots in the terminals of a T-shaped antenna, dual or triple operating bands can be achieved. In order to validate the feasibility of this method, this type of antenna is designed and simulated. The antennas are respectively fed by two different feeding transmission lines (microstrip transmission line and coplanar waveguide (CPW) transmission line) for the purpose of identifying the method that can be commonly used. The parametric analysis in detail has been given to explain the effects of the key parameter variations. For WLAN and WiMAX applications, the antennas are fabricated and measured. Both simulated and measured results are presented to demonstrate the feasibility of these designs.

1. INTRODUCTION

In modern wireless communications, it is becoming desirable to design a printed antenna covering two or three frequency bands for more and more systems and devices. For example, some handheld devices may be required to simultaneously provide wireless access services for both the wireless local area network (WLAN) and worldwide interoperability for microwave access (WiMAX). In order to reduce the quantity of connector and cost, and at the same time easily integrate with the devices, it is better for the transmitting and receiving antennas to operate in dual band or triple band.

Some researchers and scholars have done lots of work on multiple band antenna research, various types of printed antennas have been reported [1–17]. The planar monopole antenna is often adapted to realize multiple-band operation, with various structures such as letter-like shape [1–6, 12], plant-like shape [7], and fractal structures [8–11, 15–17]. An asymmetrical meandered T-shaped monopole with a long and a short arm has been used in [1], and a dual band has been realized. In [2–6], T-shaped, G-shaped, M-shaped, S-shaped, and Y-shaped antennas, which achieved triple band operation, have been reported. A miniascape-like antenna having triple band characteristics has been shown in [7]. The fractal antennas have been researched for a long time. An E-shaped fractal antenna has been reported in [8]. It combines the letter-like-shape and fractal theory to make the antenna achieve multiple band. In [9], an overview of the fractal antenna engineering has been presented, giving a brief overview of some of the more common fractal geometries and some fractal antenna elements. In [10], researchers have summarized some of the unique features of fractal geometries, and drawn conclusions about the utilization of these complicated intricate structures in manufacturable antennas. In [11], authors have provided a comprehensive overview of developments in the field of fractal antenna engineering, with particular emphasis placed on the theory and design of fractal arrays. These types of antennas have exhibited excellent characteristics including compact size, low profile, and easy integrability with systems.

Received 1 July 2014, Accepted 14 August 2014, Scheduled 22 August 2014

* Corresponding author: Tao Ni (tao_ni@hotmail.com).

The authors are with the National Key Laboratory of Antennas and Microwave Technology, Xidian University, Xi'an, Shaanxi 710071, P. R. China.

Inspired by the theory and geometries of fractal antennas, we present a method in this paper where T-shaped slots are loaded in the terminals of a T-shaped antenna. This method can make the proposed structure realize multiple band operation in comparison with the original T-shaped antenna. In order to identify the versatility of this method, two different feeding transmission lines are respectively connected with the proposed structure. The effects of the key parameters are studied so as to adjust the size of the antenna to get the desired results. These antennas are designed for WLAN and WiMAX applications and detailed parametric study are given. Both simulated and measured results for these antennas are given to verify the feasibility of this method.

2. ANTENNA DESIGN

2.1. Antenna Evolution Process

Figure 1 shows the various antennas involved in the multiple band design evolution process. The original T-shaped antenna is called Ant A, and it operates in a single frequency band. Adding double T-shaped slots into the terminals of Ant A, the dual band antenna called Ant B is achieved. Because of the two T-shaped slots, two resonant lengths exist at different frequencies and another resonant frequency occurs. Thus, the Ant B can operate in two frequency bands. Adding double T-shaped slots into the terminals of Ant B, the triple band antenna which is called Ant C is achieved. Using a similar theory, Ant C has three resonant lengths at different frequencies and it can hence operate in three frequency bands.

2.2. Two Types of Feeding Methods

The antennas are respectively fed by a microstrip transmission line and a CPW transmission line, and the schematic diagram for triple band operation is shown in Figure 2.

2.3. Simulated Results of the Antennas

The simulated results of the antennas are obtained using Ansoft High Frequency Structure Simulator (HFSS). The maximum delta energy in the software is set to 0.02. The simulation is run in a PC, with an Intel Xeon 1230 V2 3.30 GHz processor and 32 GB of RAM.

The simulated return losses ($|20 * \log 10|S_{11}||$) are shown in Figure 3. In Figure 3(a), the antennas are fed by a microstrip line. Ant A can achieve return loss > 10 dB in 5.83–6.28 GHz, Ant B can achieve return loss > 10 dB in 3.03–3.41 GHz and 5.59–5.95 GHz, and Ant C can achieve return loss > 10 dB in 2.41–2.52 GHz, 3.3–3.69 GHz, and 5.55–5.94 GHz. Results for antennas fed by a CPW transmission line are shown in Figure 3(b). Ant A can achieve return loss > 10 dB in 5.81–6.43 GHz, Ant B can achieve return loss > 10 dB in 2.98–3.41 GHz and 5.48–5.78 GHz, and Ant C can achieve return loss > 10 dB

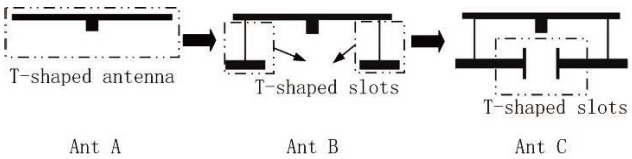

Figure 1. Design evolution process.

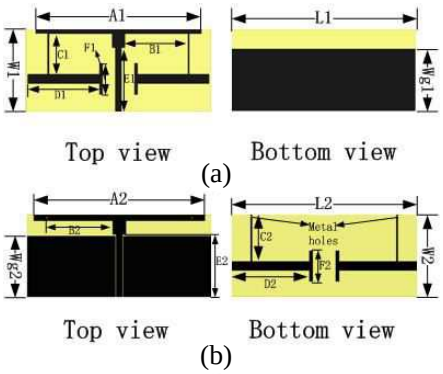

Figure 2. The schematic diagram for triple band antenna, (a) fed by microstrip line, (b) fed by CPW.

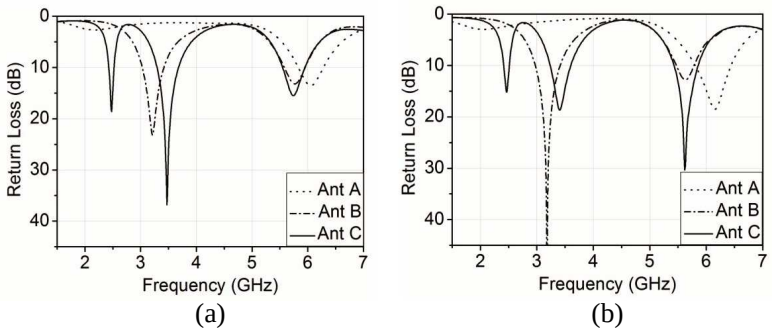

Figure 3. Simulated return losses of antennas A, B, C, (a) fed by microstrip line, (b) fed by CPW.

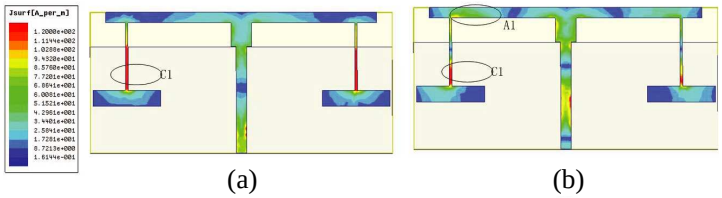

Figure 4. Surface current distributions for Ant B, (a) 3.2 GHz, (b) 5.8 GHz.

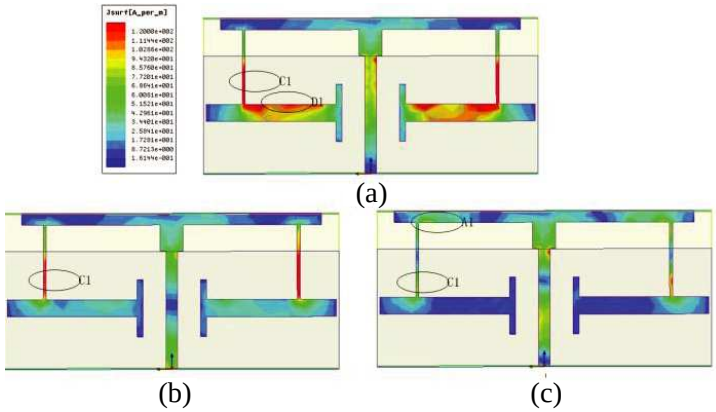

Figure 5. Surface current distributions for Ant C, (a) 2.45 GHz, (b) 3.5 GHz, (c) 5.8 GHz.

in 2.41–2.51 GHz, 3.24–3.6 GHz, and 5.43–5.86 GHz. These results show that no matter whether the antennas are fed by a microstrip line or a CPW transmission line, the varying disciplines of return loss are the same. Also, Ant Bs achieved two band characteristics, while Ant Cs achieved triple band characteristics.

2.4. Surface Current Distributions

In order to further investigate the multiple operation mechanism of the proposed antennas, the surface current distributions for Ant B and Ant C fed by a microstrip line are respectively shown in Figure 4 and Figure 5. According to Figure 4, at the resonant frequency 3.2 GHz, significant surface current density is observed by C1, and at resonant frequency 5.8 GHz, significant surface current density is observed by C1 and A1. According to Figure 5, we can draw the conclusion that the significant surface current densities for Ant C at resonant frequencies 3.5 GHz and 5.8 GHz are similar to those of Ant B. Significant surface current densities at 2.45 GHz are observed by D1 after adding double T-shaped slots in the terminals of Ant B. According to the surface current distributions for Ant B and Ant C, we can

see that the T-shaped slots loaded in the terminals of T-shaped antenna can achieve multiple band operation.

3. PARAMETRIC STUDY OF THE PROPOSED ANTENNAS

The effects of various parameters on the return loss are analyzed for further study. When one parameter is studied, the others are kept constant. The effects of parameters are respectively explored for Ant B and Ant C, while the feed method is using a microstrip line. The results provide a useful guideline for practical design.

3.1. Parametric Study for Ant B

3.1.1. The Effects of L_a & L_d

The effects of L_a and L_d on return loss are presented in Figure 6. As can be seen from Figure 6(a), when L_a is increased, the higher frequency band is obviously shifting towards lower frequencies and the lower frequency band is not changing. When L_d is extended, the higher frequency band is shifting towards higher frequencies and the lower frequency band has no obvious change. Thus, these results indicate that through changing L_a and L_d, the higher frequency band could be adjusted.

3.1.2. The Effects of L_c

Figure 7(a) illustrates how L_c influences on the frequency bands. Specifically, we can see that the lower frequency band is moving towards lower frequencies as L_c is increased, but that it does not influence

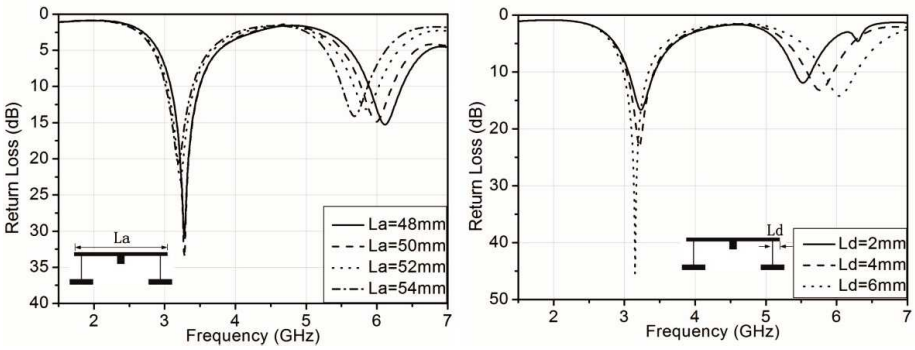

Figure 6. The effects of L_a & L_d for Ant B, (a) L_a, (b) L_d.

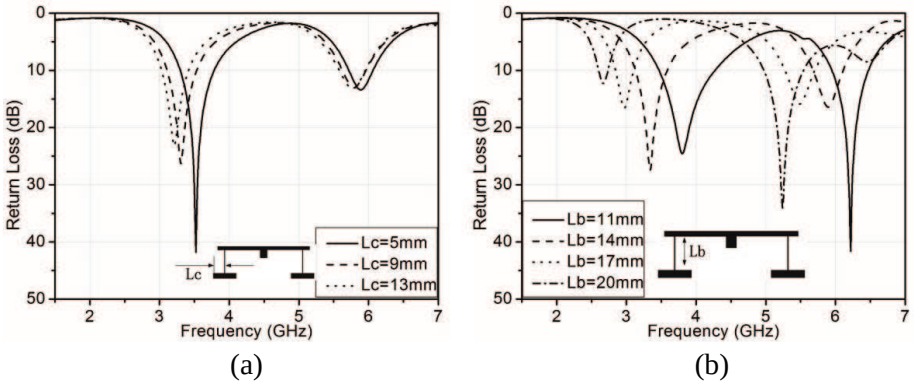

Figure 7. The effects of L_c & L_b for Ant B, (a) L_c, (b) L_b.

the higher frequency band. Thus, this shows that the lower frequency band can be adjusted by varying L_c.

3.1.3. The Effects of L_b

Figure 7(b) is mainly used to show that the dual frequency bands are shifting towards lower frequency band with L_b extended, which indicates that L_b can be used to adjust the dual frequencies.

Through the above analysis, the effects of the parameters L_a, L_b, L_c, and L_d for Ant B have been demonstrated clearly. To sum up, we can easily gain the desired dual characteristics for Ant B by adjusting these parameters as described above.

3.2. Parametric Study for Ant C

3.2.1. The Effects of L_a & L_d

Figure 8 shows the effects of L_a and L_d for Ant C. It demonstrates that the higher frequency band is obviously shifting towards lower frequencies as we increase L_a and that the other two frequency bands do not change a lot. According to Figure 8(b), with the increase of L_d, the higher frequency band is shifting towards higher frequencies, but the other two frequency bands are reluctant to change. Therefore, L_a and L_d have the effects of adjusting the higher frequency band.

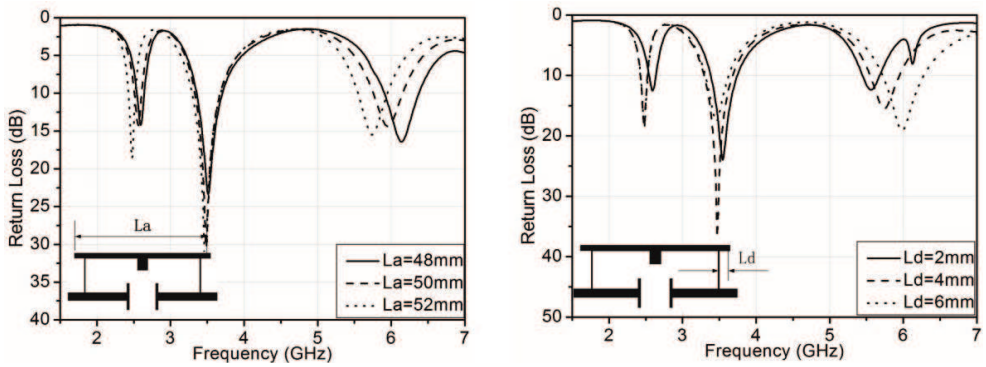

Figure 8. The effects of L_a & L_d for Ant C, (a) L_a, (b) L_d.

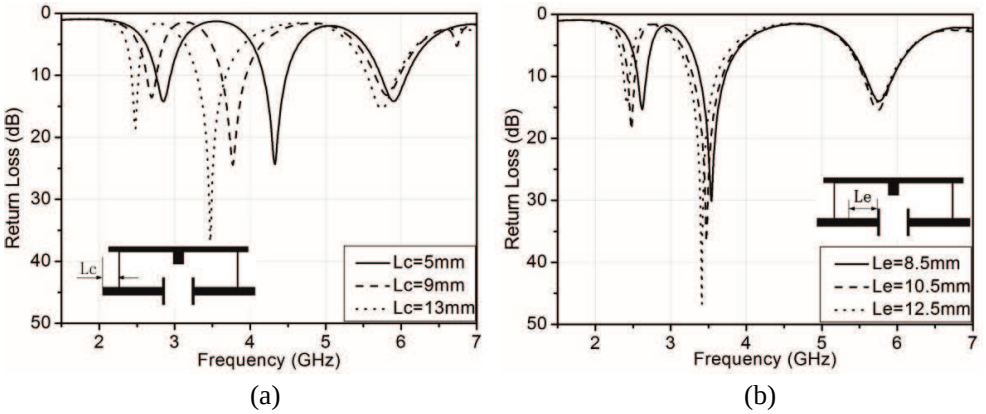

Figure 9. The effects of L_c & L_e for Ant C, (a) L_c, (b) L_e.

3.2.2. The Effects of L_c & L_e

In Figure 9, when considering the effects of L_c and L_e, the lower and middle frequency bands are moving from higher frequencies to lower frequencies when L_c or L_e increased, but no significant effect of L_c and L_e is seen on the higher frequency band. Thus, it shows that the lower and middle frequency bands can be controlled by changing parameters L_c and L_e.

3.2.3. The Effects of L_b

Effects of L_b are shown in Figure 10, and we can see clearly that all the frequency bands are shifting towards lower frequencies when we adjust L_b from 11 mm to 20 mm. In this case, it illustrates that increasing L_b can help us to adjust all three frequency bands for Ant C.

The parametric study as described above demonstrates that it is easy to obtain dual band characteristics or triple band characteristics through adjusting parameters of the proposed antenna. A detailed parametric study can provide useful guidelines for engineering applications to gain arbitrary desired multiple frequency band characteristics.

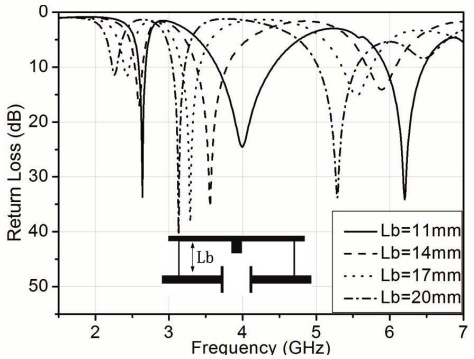

Figure 10. The effects of L_b.

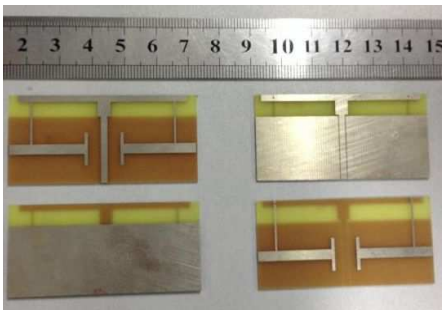

Figure 11. A photograph of proposed antenna.

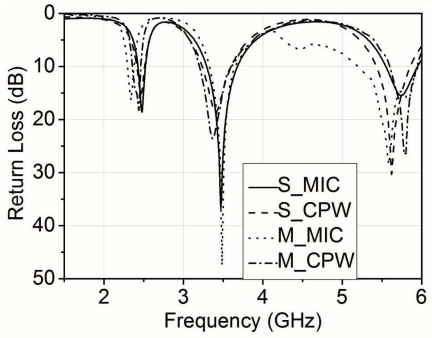

Figure 12. Simulated and measured return losses.

Table 1. The dimensions of the proposed antenna. Units: mm.

Parameters	L_1	W_1	A_1	B_1	C_1	D_1	E_1	F_1	W_{g1}
Values	58	27	52	20	13	22	20.5	10	20.5
Parameters	L_2	W_2	A_2	B_2	C_2	D_2	E_2	F_2	W_{g2}
Values	58	27	52	20	14.5	23.5	20.5	10	20

4. EXPERIMENTAL RESULTS

For WLAN and WiMAX applications, the proposed antennas fed by two different types of transmission lines are simulated and fabricated. A detailed annotation of parameters is shown in Figure 2 and the dimensions of the proposed antennas are shown in Table 1. A photograph of the proposed antenna is shown in Figure 11. The antenna on the left is fed by a microstrip line, and that on the right is fed by a CPW. The total size of the antenna fed by the microstrip is 58 mm × 27 mm × 1 mm, and the total size of antenna fed by the CPW is 58 mm × 27 mm × 1 mm.

SMA connectors of impedance 50 Ohms have been connected with the input ports of the antennas for simplicity of measurement. The return losses have been measured using Wiltron-37269A network analyzer. Figure 12 shows the simulated and measured return loss for proposed antennas, with S_MIC and S_CPW respectively representing the simulated results for microstrip transmission line and CPW transmission line, and M_MIC and M_CPW representing the corresponding measured results. Measured

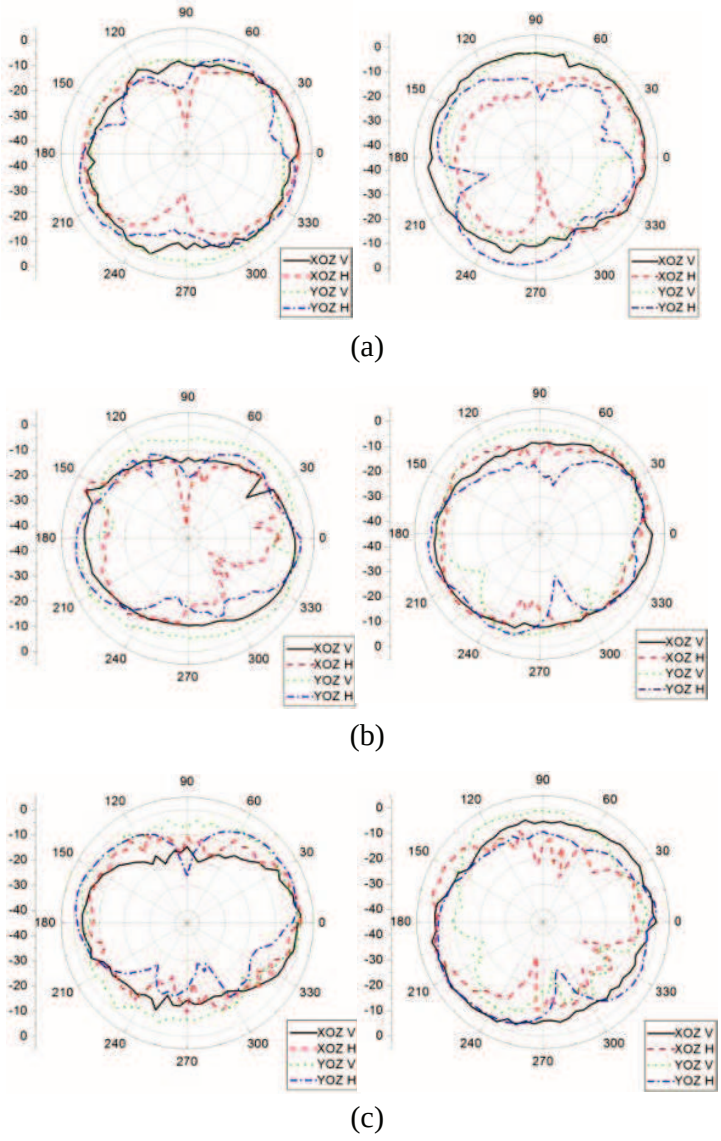

Figure 13. Measured radiation patterns at (a) 2.45 GHz, (b) 3.5 GHz, (c) 5.8 GHz. Patterns on the left are for an antenna fed by a CPW, and those on the right are for an antenna fed by a microstrip line.

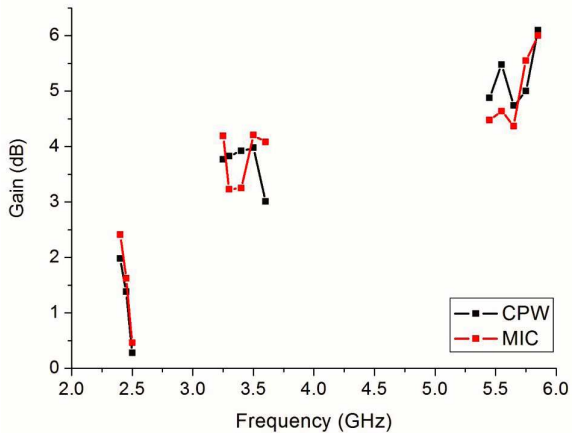

Figure 14. Measured peak gains.

results, M_MIC shows that the antenna can achieve triple band operation in 2.35–2.45 GHz, 3.2–3.6 GHz, 5.2–5.94 GHz, and M_CPW shows that the antenna can achieve triple band operation in 2.4–2.5 GHz, 3.35–3.7 GHz, 5.6–5.97 GHz. The differences between simulated and measured results are caused by manufacturing errors. Ignoring the effects of SMA connectors on the simulated and measured return losses have caused large differences in the higher frequency band, especially in M_MIC and S_MIC. The measured radiation patterns of the proposed antennas at 2.45 GHz 3.5 GHz, and 5.8 GHz are shown in Figure 13. The measured peak gains are given in Figure 14, which shows that the average gains for microstrip transmission line feed method are 1.5, 3.79, and 5 dB, for the lower, middle, and upper bands, respectively, and the average gains for CPW-feeding are 1.21, 3.7, and 5.2 dB, respectively. The measured results prove that the proposed antennas are suitable for simultaneous WLAN/WiMAX applications. Compared with antennas in other references, the advantages of the proposed antenna are listed as follows: 1) the antenna's performance is independent of the feed methods. Two types of feed methods have been used in this design to prove it; 2) the structure for this design is simple and it is easy to gain arbitrary desired multiple frequency band characteristics.

5. CONCLUSION

A method where a T-shaped antenna loading T-shaped slots for multiple band operation has been presented in this paper. The proposed T-shaped antenna with T-shaped slots loaded in the terminals can operate in multiple bands instead of only one band realized when using the original T-shaped antenna. The design evolution process and surface current distributions are given to show how to achieve dual or triple operating band characteristics. A microstrip and a CPW transmission line are respectively used for the purpose of proving that the method can be commonly used for multiple band wireless terminal systems. A parametric analysis has been conducted to prove this antenna can achieve multiple operation bands through adjusting of antenna parameters. The triple band antennas for WLAN /WiMAX application systems fed by two types of methods have been fabricated and measured. Good impedance matching, almost omni-directional radiation patterns and stable antenna gains across the operating bands have demonstrated that this proposed antenna can be regarded as a potential candidate for WLAN/WiMAX application systems. To sum up, this proposed antenna is very easy to fabricate, and very attractive for current and future communication system applications.

REFERENCES

1. Chang, T. N. and J.-H. Jiang, "Meandered T-shaped monopole antenna," *IEEE Trans. Antennas Propag.*, Vol. 57, No. 12, 3976–3978, 2009.
2. Hu, W., Y.-Z. Yin, X. Yang, and P. Fei, "Compact multiresonator-loaded planar antenna for multiband operation," *IEEE Trans. Antennas Propag.*, Vol. 61, No. 5, 2838–2841, 2013.

3. Song, Y., Y.-C. Jiao, H. Zhao, Z. Zhang, Z.-B. Weng, and F.-S. Zhang, "Compact printed monopole antenna for multiband WLAN applications," *Microw. Opt. Technol. Lett.*, Vol. 50, No. 2, 365–367, 2008.
4. Peng, L., C.-L. Ruan, and X.-H. Wu, "Design and operation of dual/triple-band asymmetric M-shaped microstrip patch antennas," *IEEE Antennas and Wireless Propag. Lett.*, Vol. 9, 1069–1072, 2010.
5. Liu, W.-C., W.-R. Chen, and C.-M. Wu, "Printed double S-shaped monopole antenna for wideband and multiband operation of wireless communications," *IEE Proceedings Microwaves Antennas and Propag.*, Vol. 151, No. 6, 473–476, 2004.
6. Liu, W.-C. and C.-F. Hsu, "Dual-band CPW-fed Y-shaped monopole antenna for PCS/WLAN application," *Electron. Lett.*, Vol. 41, No. 7, 390–391, 2005.
7. Deng, C.-P., X.-Y. Liu, Z.-K. Zhang, and M. M. Tentzeris, "A miniascape-like triple-band monopole antenna for WBAN applications," *IEEE Antennas and Wireless Propag. Lett.*, Vol. 11, 1330–1333, 2012.
8. Bayatmaku, N., P. Lotfi, M. Azarmanesh, and S. Soltani, "Design of simple multiband patch antenna for mobile communication applications using new E-shape fractal," *IEEE Antennas and Wireless Propag. Lett.*, Vol. 10, 873–875, 2011.
9. Werner, D. H. and S. Ganguly, "An overview of fractal antenna engineering research," *IEEE Antennas and Propag. Mag.*, Vol. 45, No. 1, 38–57, 2003.
10. Gianvittorio, J. P. and Y. Rahmat-Samii, "Fractal antennas: A novel antenna miniaturization technique, and applications," *IEEE Antennas and Propag. Mag.*, Vol. 44, No. 1, 20–36, 2002.
11. Werner, D. H., R. L. Haupt, and P. L. Werner, "Fractal antenna engineering: The theory and design of fractal antenna arrays," *IEEE Antennas and Propag. Mag.*, Vol. 41, No. 5, 37–58, 2002.
12. Zhao, G., F.-S. Zhang, Y. Song, Z.-B. Weng, and Y.-C. Jiao, "Compact ring monopole antenna with double meander lines for 2.4/5 GHz dual-band operation," *Progress In Electromagnetics Research*, Vol. 72, 187–194, 2007.
13. Sze, J.-Y., T.-H. Hu, and T.-J. Chen, "Compact dual-band annular-ring slot antenna with meandered grounded strip," *Progress In Electromagnetics Research*, Vol. 95, 299–308, 2009.
14. Wu, Y.-J., B.-H. Sun, J.-F. Li, and Q.-Z. Liu, "Triple-band omni-directional antenna for WLAN application," *Progress In Electromagnetics Research*, Vol. 76, 477–484, 2007.
15. Mahatthanajatuphat, C., S. Saleekaw, P. Akkaraekthalin, and M. Krairiksh, "A rhombic patch monopole antenna with modified Minkowski fractal geometry for UMTS, WLAN, and mobile WiMAX application," *Progress In Electromagnetics Research*, Vol. 89, 57–74, 2009.
16. Mahatthanajatuphat, C., P. Akkaraekthalin, S. Saleekaw, and M. Krairiksh, "A bidirectional multiband antenna with modified fractal slot fed by CPW," *Progress In Electromagnetics Research*, Vol. 95, 59–72, 2009.
17. Jalil, M. E. B., M. K. A. Rahim, N. A. Samsuri, N. A. Murad, H. A. Majid, K. Kamardin, and M. A. Abdullah, "Fractal Koch multiband textile antenna performance with bending, wet conditions and on the human body," *Progress In Electromagnetics Research*, Vol. 140, 633–652, 2013.